



Available online at www.sciencedirect.com

SCIENCE @ DIRECT®

C. R. Geoscience 335 (2003) 1039–1048



Surface Geosciences (Hydrology–Hydrogeology)

Strontium, $\text{SO}_4^{2-}/\text{Cl}^-$ and $\text{Mg}^{2+}/\text{Ca}^{2+}$ ratios as tracers for the evolution of seawater into coastal aquifers: the example of Castell de Ferro aquifer (SE Spain)

Pablo Pulido-Leboeuf^a, Antonio Pulido-Bosch^{a,*}, Maria Luisa Calvache^b,
Ángela Vallejos^a, José Miguel Andreu^c

^a Department of Hydrogeology and A.C., University of Almería, 04120 La Cañada, Almería, Spain

^b Department of Geodynamics, University of Granada, Campus Fuentenueva, 18071 Granada, Spain

^c Department of Earth and Environmental Science, P.O. Box 99, 03080 Alicante, Spain

Received 19 February 2001; accepted 11 August 2003

Presented by Ghislain de Marsily

Abstract

The strontium content and the $\text{SO}_4^{2-}/\text{Cl}^-$ and $\text{Mg}^{2+}/\text{Ca}^{2+}$ ratios were used as natural tracers of the residence time of seawater intrusion into the Castell de Ferro aquifer. Analysis of these parameters indicated the existence of two principal flowpaths in the aquifer. The first flows through the eastern part of the aquifer, through the karstified Castell de Ferro massif; it accommodates a larger and more rapid flow, so that the residence time is shorter, leading to lower $\text{SO}_4^{2-}/\text{Cl}^-$ ratios, lower Sr^{2+} content and higher $\text{Mg}^{2+}/\text{Ca}^{2+}$ ratios. The second flowpath is in the western sector, and flows exclusively through alluvial deposits; the flow here is slower, particularly that flowing towards the sea. Thus the residence time of the water here will be longer and there is scant flushing of the intruded seawater; this is manifested in the high Sr^{2+} content, high $\text{SO}_4^{2-}/\text{Cl}^-$ and low $\text{Mg}^{2+}/\text{Ca}^{2+}$ ratios. **To cite this article:** P. Pulido-Leboeuf et al., C. R. Geoscience 335 (2003).

© 2003 Académie des sciences. Published by Elsevier SAS. All rights reserved.

Résumé

Strontium, et rapports $\text{SO}_4^{2-}/\text{Cl}^-$ et $\text{Mg}^{2+}/\text{Ca}^{2+}$ en tant que traceurs de l'évolution de l'eau de mer dans les aquifères côtiers : exemple de Castell de Ferro (Sud-Est de l'Espagne). La teneur en Sr^{2+} et les rapports $\text{SO}_4^{2-}/\text{Cl}^-$ et $\text{Mg}^{2+}/\text{Ca}^{2+}$ ont été utilisés comme traceurs naturels du temps de résidence de l'eau de mer dans l'aquifère de Castell de Ferro. On déduit, à partir de l'analyse de ces paramètres, l'existence de deux voies principales d'écoulement dans l'aquifère. L'une se situe dans la partie la plus orientale, à travers le massif karstifié de Castell de Ferro, où l'écoulement est élevé et rapide. Le temps de transit est donc court; ces eaux sont caractérisées par de faibles valeurs du rapport $\text{SO}_4^{2-}/\text{Cl}^-$ et de faibles teneurs en Sr^{2+} . L'autre, dans le secteur plus occidental, transite exclusivement par des matériaux détritiques, où l'écoulement est plus lent. Le temps de résidence y est plus élevé et le processus d'extrusion d'eau de mer plus faible. Ces eaux ont des

* Corresponding author.

E-mail addresses: ppulido@ual.es (P. Pulido-Leboeuf), apulido@ual.es (A. Pulido-Bosch), calvache@ugr.es (M.L. Calvache), avallejo@ual.es (A. Vallejos), andreurodes@ua.es (J.M. Andreu).

teneurs élevées en Sr^{2+} , des valeurs élevées du rapport $\text{SO}_4^{2-}/\text{Cl}^-$ et des valeurs faibles du rapport $\text{Mg}^{2+}/\text{Ca}^{2+}$. **Pour citer cet article :** P. Pulido-Leboeuf et al., C. R. Geoscience 335 (2003).

© 2003 Académie des sciences. Published by Elsevier SAS. All rights reserved.

Keywords: seawater intrusion; residence time; natural tracers; preferential flow; water–rock interaction

Mots-clés : intrusion d'eau de mer ; temps de résidence ; traceurs naturels ; écoulement préférentiel ; interaction eau–roche

Version française abrégée

L'aquifère de Castell de Ferro est situé au Sud de l'Espagne (Fig. 1) où règne un climat semi-aride à saison sèche prononcée. La période de pompage maximum coïncide avec celle de moindre disponibilité en ressources hydriques. La grande rentabilité des cultures sous serres de la région provoque la surexploitation de l'aquifère de Castell de Ferro, avec un processus d'intrusion saline [3,8]. Il s'agit d'un aquifère détritique d'environ 3 km^2 , de forme allongée, d'environ 5 km de long et d'un maximum de 700 m de large. La précipitation moyenne annuelle à la station de Motril est de 384 mm. L'évapotranspiration potentielle est très supérieure à la précipitation annuelle (940 mm) [11].

Les matériaux préorogéniques qui affleurent dans la zone sont des métapélites et des marbres du Complexe Alpujarride [1]. L'aquifère est composé de dépôts alluviaux qui occupent le fond des lits secs (« ramblas ») et leur embouchure (Fig. 2). Ils sont composés de graviers, sables, limons et argiles et atteignent environ 60 m d'épaisseur. L'existence de deux affleurements carbonatés, en contact avec l'aquifère et avec la mer, a une grande importance sur le fonctionnement du système [6]. Les valeurs de transmissivité sont comprises entre 0,003 et $0,12 \text{ m}^2/\text{s}$ et sont distribuées de façon telle, que les valeurs maximales se trouvent sur l'axe de la rambla, dans la zone la plus proche de la côte, et diminuent vers les bords de la rambla et en amont [5]. Le flux se produit dans le sens nord-sud, avec un gradient moyen de près de 2‰. L'exploitation intensive de l'aquifère dans le but de satisfaire la demande des cultures sous serres a provoqué l'apparition temporaire d'inversion du gradient, avec des niveaux piézométriques au-dessous du niveau de la mer [4]. À partir de la fin des années 90, l'irrigation se fait avec de l'eau à faible teneur en sel (moins de 500 mg/l) provenant de la rivière Guadalfeo (Fig. 1). Le système d'irrigation dominant est d'efficacité élevée (goutte à goutte).

On a prélevé un total de 33 échantillons le 25 novembre 1998 et le 25 mars 1999. Les prélèvements ont été effectués par pompage ou avec un hydrocapteur mécanique à ouverture contrôlée. Le Tableau 1 montre les résultats analytiques et leurs erreurs de bilan analytique respectives. Le diagramme de Piper de la Fig. 3 représente les résultats des analyses chimiques des eaux. Il existe un alignement principal qui montre une gradation qui va du faciès HCO_3-Ca au faciès $\text{Cl}-\text{Na}$ et un alignement secondaire à plus grande proportion en SO_4^{2-} . La matrice de corrélation (Tableau 2) met en évidence le rapport existant dans le groupe de variables représentant la salinité (conductivité électrique, Cl^- , SO_4^{2-} , Na^+ , K^+ , Ca^{2+} , Mg^{2+} , Sr^{2+} et B). D'autre part, les autres variables (température, pH, HCO_3^- , NO_3^- et SiO_2) montrent une faible corrélation entre elles, due à la disparité de leurs origines. Le rapport $\text{SO}_4^{2-}/\text{Cl}^-$ [12] diminue lorsque la proportion d'eau de mer dans le mélange augmente, représentée par la teneur en Cl^- (Fig. 4). Trois échantillons s'éloignent de la tendance générale, en raison de leurs faibles teneurs en Cl^- et des faibles valeurs du rapport $\text{SO}_4^{2-}/\text{Cl}^-$ (environ 0,2). Ces trois échantillons ont été prélevés dans des forages qui captent l'eau des matériaux métapélitiques situés à l'ouest de l'aquifère détritique. On distingue deux alignements; le plus dense est distribué selon la fonction $y = 1,4334 x^{-0,4763}$ ($R^2 = 0,9423$), tandis que celui qui montre une plus grande valeur du rapport $\text{SO}_4^{2-}/\text{Cl}^-$ a été ajusté selon la fonction $y = 2,6482 x^{-0,5212}$ ($R^2 = 0,9655$), avec y le rapport $\text{SO}_4^{2-}/\text{Cl}^-$ et x la concentration en Cl^- en meq/l. Les eaux de ce deuxième alignement présentent un apport supplémentaire en SO_4^{2-} , dû sûrement à la dissolution de petites quantités de gypse éparpillé au sein de l'aquifère et provenant des matériaux métapélitiques, et à un plus grand temps de résidence. Le rapport $\text{Mg}^{2+}/\text{Ca}^{2+}$ [14] augmente en fonction de la proportion d'eau de mer introduite dans le mélange (Fig. 5); mais, dans l'échantillon 3–50 m et dans les autres

échantillons à teneur élevée en $\text{SO}_4^{2-}/\text{Cl}^-$, elle est plus faible que dans les autres, en raison d'un processus d'échange entre Ca^{2+} et Na^+ , favorisé par l'intrusion et par le temps de résidence plus élevé. L'ion Sr^{2+} montre une augmentation progressive de sa concentration, parallèlement à l'augmentation en ions chlorure (Fig. 6). Sa concentration peut augmenter par rapport au mélange théorique eau douce-eau de mer, par suite de la dissolution de la matrice. Cette augmentation met en évidence un temps de résidence plus élevé [10,13], comme il se produit pour l'échantillon 3–50 m et pour ceux à teneur élevée en $\text{SO}_4^{2-}/\text{Cl}^-$. Ces échantillons (3–50 m, 3–30 m, 4–30 m, 5, 8 et 2) représentent une zone de l'aquifère où l'eau de mer a été très peu lessivée. Tout ceci est plus évident dans l'échantillon qui présente une plus grande proportion en eau de mer (3–50 m). Les points concernés se trouvent dans la partie occidentale de l'aquifère détritique, déplacés par rapport au lit de la rambla. Les eaux captées dans ces puits et forages montrent une zone de plus faible écoulement vers la mer, étant donné qu'il s'agit d'une voie secondaire d'écoulement souterrain dans l'aquifère de Castell de Ferro. Par contre, les forages et puits plus proches du bloc carbonaté se trouvent dans la voie préférentielle de l'écoulement souterrain, ce qui fait que les processus de mélange eau douce-eau de mer [2] dominant tous les autres processus modificateurs, ceci étant dû au moindre temps de résidence que dans l'autre secteur de l'aquifère.

1. Introduction

A general feature of coastal areas is their large water demand, because of the fact that they are usually densely populated and subject to intensive agriculture and tourism. The intensive exploitation of coastal aquifers in an attempt to satisfy this demand may generate problems due to marine intrusion. In addition, both agricultural activities and urban settlements tend to be situated over water bearing materials, which greatly increases the risk of groundwater pollution.

The Castell de Ferro aquifer is located in the south of Spain, where a semiarid Mediterranean climate prevails. The dry season is pronounced and this aggravates the situation, given that the highest water demand usually coincides with the period of least availability of water (dry weather conditions). The main

problems in the aquifers of the region arise as a result of the intensive exploitation, agricultural activities, the existence of highly-soluble minerals (gypsum dispersed through the rock) and the mobilization of brackish connate waters, or waters derived from the saturation of semi-permeable materials by seawater during former sea level regimes.

The principal aim of this study was to characterize the hydrogeochemistry of these coastal aquifers, identifying the main processes that occur in the system. Specifically, the study aimed to determine the extent of marine intrusion in the aquifer, and confirm whether we are dealing with a single intrusion phenomenon or the superimposition of different processes of seawater intrusion. To achieve this aim, the concentration of Sr^{2+} in the water was studied, along with some ionic ratios.

2. Hydrogeological settings

The Castell de Ferro aquifer system undergoes the consequences of overexploitation caused by the introduction of greenhouse crops during the 1980s [3,8]. The dominant cultivation in the area is market garden crops grown under plastic, and these occupy almost all of the area of the aquifer, and are even invading the neighbouring hillsides, through the removal of the less competent metapelitic materials. These crops prove a high water use efficiency, as they are drip-irrigated. The study area lies at the eastern coast of Andalusia. It is a detrital aquifer linked to the deposits of the Ancha and de Gualchos *ramblas* (dry stream beds), and it occupies a surface area of more than 3 km². Its form is north–south elongated, measuring some 5 km long and up to 700 m wide. The aquifer is surrounded by a mountainous relief, except to the south where it is limited by the Mediterranean Sea (Fig. 1). The prevailing climate in the region is semi-arid temperate Mediterranean, with a mean annual temperature of 18.9 °C, a minimum of 9.2 °C in January and a maximum of 30.8 °C in August. The mean annual precipitation in the area is about 380 mm. Potential evapotranspiration (940 mm) greatly exceeds the annual precipitation [11].

Pre- and post-orogenic materials outcrop in the study area (Fig. 2). The former belong to the Alpujarride Complex and are metapelites belonging to the Adra and Murtas units; the Murtas rocks contain some

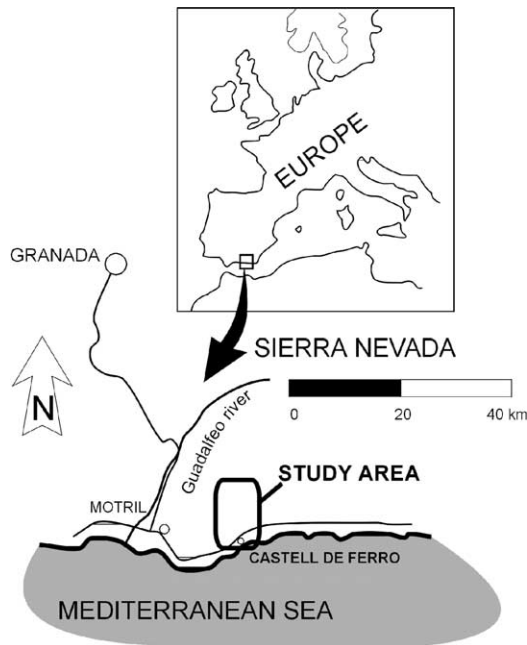


Fig. 1. Geographic situation of the study area.

Fig. 1. Situation géographique de la zone d'étude.

fairly disperse intercalations of limestone and gypsum. The Murtas unit also contains marble [1]. The alluvial deposits that fill the bottom of the ramblas are the post-orogenic materials that occupy the greatest surface. They are composed of gravels, sands, silts and clays. The maximum thickness reached by these deposits in boreholes is some 60 m near the confluence of the two ramblas. There are also small outcrops of encrusted layers and cemented conglomerates, which comprise former river beds and outwash cones, respectively. The presence of two carbonate outcrops in contact with the aquifer and with the sea plays an important role in the behaviour of the system, as they can serve as preferential flow paths in the exchange of water between the aquifer and the sea [6].

The catchment area of the Gualchos rambla is nearly 80 km² and it is developed mainly over metapelitic materials. These materials favour the generation of run-off that flows along the ramblas, which have a high infiltration capacity. Transmissivity of the aquifer ranges between 0.003 and 0.12 m²/s; the maximum values are recorded along the axis of the rambla and in the area closest to the coast, whilst the values decrease towards the banks of the rambla and towards its headwaters [5]. The direction of flow is north to

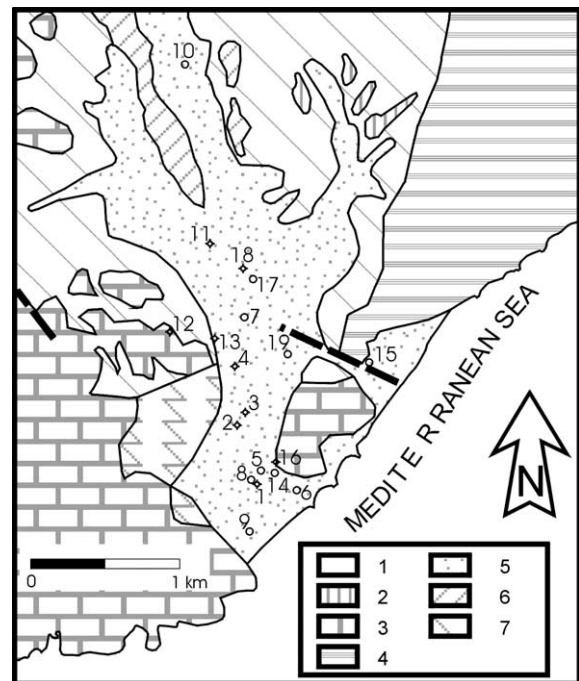


Fig. 2. Geological scheme of the study area indicating the sampling points. 1: metapelites of the Murtas unit; 2: limestone intercalations in the Murtas metapelites; 3: marble of the Murtas unit; 4: metapelites of the Adra unit; 5: alluvia; 6: conglomerates; 7: cemented conglomerates.

Fig. 2. Cadre géologique de la zone d'étude, avec indication des points de prélèvements d'eau. 1 : métapélites de la nappe de Murtas ; 2 : intercalations calcaires au sein des métapélites de la nappe de Murtas ; 3 : marbres de la nappe de Murtas ; 4 : métapélites de la nappe d'Adra ; 5 : sédiments alluviaux ; 6 : conglomérats ; 7 : conglomérats cimentés.

south, with a mean slope close to 2%. The section in which pumping is concentrated is that of Vega de Castell, situated approximately 1 km from the coast. The intensive exploitation of the aquifer to satisfy the demand of the greenhouses leads to seasonal piezometric levels below sea level [4]. This problem seems to have diminished at present due to a recent water transfer scheme bringing water with TDS lower than 500 mg/l from the neighbouring catchment of the River Guadalfeo.

3. Methods

This article presents the results of two sampling surveys undertaken at different times during the same hydrologic year. A total of 33 samples were taken

over the two sampling runs, made on 25 November 1998 and 25 March 1999. Most of the samples were pumped, although some of those collected during November 1998 were collected using a bailer, which was used in the monitoring well to take samples at various depths. Sixteen samples were taken from large diameter hand-dug wells, slotted along their entire length. Eight of these sixteen samples were taken from wells that cross the entire aquifer thickness, whilst the other seven were taken from shallow wells, since they were taken from the coastal strip; a further six samples were taken from cable tool drilling boreholes crossing the entire aquifer thickness, whilst the remaining eleven samples were taken from small-diameter boreholes penetrating the whole aquifer thickness. The latter were drilled by cable tool drilling in the detrital aquifer and by down-hole hammer drilling in the carbonate materials.

Electrical conductivity, temperature and pH were measured in situ. Two aliquots were taken, one for cation analysis and the other for anion analysis; 0.25 ml/l of HNO₃ was added to the first set to prevent precipitation of Na⁺, K⁺, Ca²⁺, Mg²⁺. The samples were kept refrigerated at 4 °C until their determinations. Bicarbonates were determined by acidimetric 0.02 N HCl titration (686 Titroprocessor METHROM), in the laboratory of the Department of Hydrogeology and Analytical Chemistry of the University of Almeria. The cations (Na⁺, K⁺, Ca²⁺, Mg²⁺ and Sr²⁺) were analysed in the laboratory of the Department of Chemical Engineering at the University of Alicante by ICP-MS; Cl⁻ was determined using AgNO₃, whilst NO₃⁻, SO₄²⁻ and B were determined spectrophotometrically.

4. Results

The analytical results are shown in Table 1, with their respective analytical errors based on the Electro Neutrality of samples. The higher EC values are reached in the deeper samples from the boreholes. EC also increases with the proximity of the well to the sea. The Piper diagram in Fig. 3 shows all the samples. A clear gradation can be seen from a calcium bicarbonate type to that of sodium chloride. The alignment is very clear, particularly in the anion triangle. An-

other, more open alignment, is also highlighted, which is characterized by a greater proportion of sulphate.

The correlation matrix (Table 2) emphasises the close relationship that exists between some variables directly related to salinity (electrical conductivity, Cl⁻, SO₄²⁻, Na⁺, K⁺, Ca²⁺, Mg²⁺, Sr²⁺ and B). The SO₄²⁻/Cl⁻ [12] ratio (in meq/l) decreases as the seawater proportion in the mixture – represented by chloride content in meq/l – increases (Fig. 4). Three samples deviate from this general trend because of their low Cl⁻ content and low SO₄²⁻/Cl⁻ ratio (about 0.2). This anomaly indicates that the SO₄²⁻ content of these samples may have varied as a result of a reduction process in this area. These three samples were taken from boreholes that tap water from the metapelitic materials at the western end of the detritic aquifer. Two functions were fitted to the rest of the samples as two branches can be easily distinguished. The first function ($y = 1.4334x^{-0.4763}$ ($R^2 = 0.9423$)), where y is the SO₄²⁻/Cl⁻ ratio and x the Cl⁻ content in meq/l includes the majority of the water samples that tend to have a lower SO₄²⁻/Cl⁻ ratio. The second function ($y = 2.6482x^{-0.5212}$ ($R^2 = 0.9655$)) was fitted to the samples that fall along a line of higher SO₄²⁻/Cl⁻. The second alignment indicates a supplementary source of SO₄²⁻, possibly due to the dissolution of small quantities of gypsum (dispersed within the heart of the aquifer and derived from the metapelitic materials) on account of the longer residence time.

The Mg²⁺/Ca²⁺ ratio (in meq/l) increases with the proportion of sea water in the mixture [9,14], since the Mg²⁺/Ca²⁺ ratio of sea water is close to 5 whilst in freshwaters it tends to be less than 1. All the samples with a Mg²⁺/Ca²⁺ ratio higher than 1 were taken from the coastal sector. In all the samples where Cl⁻ concentrations exceeded 10 meq/l, there was a higher Mg²⁺ than Ca²⁺ content, except for sample 3–50 m (Fig. 5). The latter result is due to cation exchange. The remaining samples have a high SO₄²⁻/Cl⁻ ratio and so the process is less evident because of the lower proportion of sea water in the mixture. However, it can be seen that the Mg²⁺/Ca²⁺ values are lower than in other samples with the same Cl⁻ content. In general, the increase in the concentration of the Sr²⁺ ion parallels that of chloride (Fig. 6), because its origin is largely due to the seawater intrusion process. Nevertheless, its

Table 1

Results of the water sample analysis. Ions expressed as mg/l; error as %

Tableau 1

Résultats analytiques des échantillons d'eau étudiés. Ions exprimés en mg/l ; erreur en %

Position	Date	E.C. ($\mu\text{S}/\text{cm}$)	T ($^{\circ}\text{C}$)	pH	Cl^{-}	Na^{+}	K^{+}	Ca^{2+}	Mg^{2+}	HCO_3^{-}	NO_3^{-}	SO_4^{2-}	SiO_2	B	Sr^{2+}	Error
1–20 m	Nov-98	2410	19.7	7.56	544	313	16.6	83	81	392.3	68	190	14.9	0.18	1.32	–4.2
1–40 m	Nov-98	27300	19.5	7.03	10500	5270	120	820	990	266.2	50	1380	15.1	0.72	14.6	3.5
1–55 m	Nov-98	47600	19.4	7.18	17995	10755	324.5	457	1099	234.2	7.8	2609	12.9	2.64	29.2	1.97
2	Nov-98	2080	20.1	7.46	302	170	2.3	183	92	352.3	270	301	26.9	0.24	1.66	–2.55
3–30 m	Nov-98	1270	19.6	7.35	161	50	16.4	219	52	379.9	68.3	305	22.9	0.23	2.75	–2.09
3–50 m	Nov-98	4580	19.4	7.3	1370	892	32.9	242	96	386.5	63.4	650	23.5	0.58	20	–0.25
4–30 m	Nov-98	1315	20.1	7.3	142	211	7.7	107	50	391.4	119.8	314	27	0.22	1.17	–1.34
7	Nov-98	995	25.8	7.54	62	57	1.8	94	41	364.3	68.8	100	22.4	0.18	0.78	–3.16
9	Nov-98	2610	20.5	7.44	586	444	6	105	65	377.5	147.8	268	22.9	0.45	1.83	–1.6
10	Nov-98	842	18	7.44	50	44	1.4	92	34	310.32	37	106	21.2	0.19	0.75	–1.77
11	Nov-98	1340	19.2	7.43	153	102	3.1	119	55	392.8	123.3	134	27.3	0.23	1.16	–3.43
12	Nov-98	763	21.5	7.41	86	54	0.7	94	10	295.83	6.8	18	23.4	0.24	0.53	–1.53
16–35 m	Nov-98	1328	18.9	7.6	221	139	7.6	92	49	331.1	41.2	132	14.7	0.09	0.88	–1.69
16–42 m	Nov-98	12570	19.2	7.38	4059	2544	70.9	228	297	323.8	46.5	722	14.3	0.61	5.27	4.33
16–44 m	Nov-98	21300	19.2	7.3	7531	4483	122.9	328	505	310.1	36.1	877	12.6	1.06	10.33	3.92
16–65 m	Nov-98	49600	19.1	7.31	19756	10775	339.5	504	1089	222	3.4	3001	11.5	2.92	29.8	–2.61
17	Nov-98	750	18.6	7.53	47	26	4.9	118	21.3	311.8	28.4	102	22.6	0.17	0.53	–2.69
18	Nov-98	805	15.8	7.82	56	42	1.6	91	33	331.35	36.4	100	21.1	0.17	0.72	–4.72
19	Nov-98	815	18.6	8.2	78	48	4	94	34	294.7	33.2	111	17.4	0.2	1.05	–2.51
2	Mar-99	2300	21.3	7.39	279	130	1.9	251	73	323.3	268.5	302	26.6	0.24	1.33	–0.05
5	Mar-99	2580	17.3	7.33	293	154	3.3	228	122	323.5	388.5	395	25.8	0.24	1.83	–0.5
6	Mar-99	1533	18.4	7.41	222	143	9.1	78	53	329.4	49.8	145	23.6	0.26	0.82	–3.96
7	Mar-99	1233	16.6	7.45	115	77	2.4	130	49	368.2	89.5	118	22.8	0.18	0.78	1.27
8	Mar-99	1669	20.8	7.28	187	200	2.6	116	40	335.5	142	234	23.6	0.26	1.42	–1.3
10	Mar-99	928	17.9	7.45	55	52	1.8	109	42	380.2	35.2	113	21.9	0.18	0.75	0.61
12	Mar-99	1011	21.3	7.27	151	82	1	113	15	321.6	8.4	21	28	0.19	0.65	–0.67
13	Mar-99	823	30.5	7.13	91	63	0.7	102	13	312.8	11.2	25	27.3	0.19	0.51	0.41
14	Mar-99	1585	18	7.54	241	154	7	83	50	320.1	49.3	146	24.3	0.25	0.9	–3.66
15	Mar-99	2900	16.4	7.6	463	324	5	165	101	541.2	198.8	227	31.1	0.37	1.56	0.55
16	Mar-99	1459	20.1	7.32	214	136	8.7	92	47	320.1	50.3	135	22.5	0.23	0.88	–2.35
17	Mar-99	885	17.9	7.35	61	36	5.4	105	24	309.4	42.4	90	21.9	0.17	0.54	–4.21
18	Mar-99	1001	16.2	7.73	58	31	1.4	105	52	326	46.4	115	21.3	0.17	0.61	2
19	Mar-99	1039	18.9	7.55	79	49	2.3	128	40	345.7	76.1	126	22.1	0.17	0.8	–0.98

concentration may be increased beyond the theoretical freshwater-sea water mixing line. This demonstrates that it can be affected by other processes. The same anomalies also appear in this graph. As well as the general increasing trend of Sr^{2+} as a function of the Cl^{-} content, one can observe that the samples corresponding to boreholes 2, 3, 5 and 8 show an elevated Sr^{2+} content in comparison to their Cl^{-} content, whilst samples from boreholes 12 and 13 have a lower Sr^{2+} content. From this, it can be deduced that the aquifer waters have not been in contact with the rock matrix for the same length of time, with three

groups being distinguished. Greater Sr^{2+} enrichment has been reported from other coastal aquifers, as a result of a longer residence time [10,13].

Examination of the $\text{SO}_4^{2-}/\text{Cl}^{-}$ and $\text{Mg}^{2+}/\text{Ca}^{2+}$ ionic ratios, as well as Sr^{2+} content leads to the conclusion that there is a clear relationship between these parameters and the Cl^{-} content, i.e., that they are indicative of the degree of mixing between fresh and saltwater in the groundwaters of the Castell de Ferro aquifer. However, some samples do not follow this general trend and these samples come from different geographical locations. On the one hand, samples 12

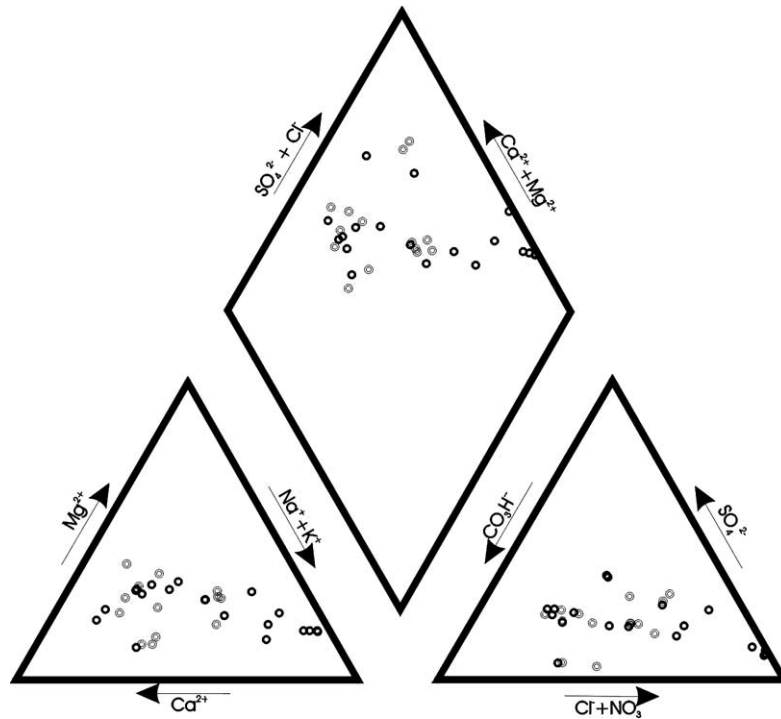


Fig. 3. Piper diagram of the water samples.
 Fig. 3. Représentation en diagramme de Piper des eaux analysées.

Table 2
 Correlation matrix of the analysed parameters

Tableau 2
 Matrice de corrélation des variables analysées

	Cond	temp	pH	Cl ⁻	HCO ₃ ⁻	SO ₄ ²⁻	NO ₃ ⁻	SiO ₂	B	Na ⁺	K ⁺	Ca ²⁺	Mg ²⁺	Sr ²⁺
Cond		-0.039	-0.388	0.999	-0.555	0.984	-0.239	-0.666	0.965	0.999	0.990	0.802	0.978	0.918
temp			-0.381	-0.034	-0.130	-0.058	-0.114	0.162	-0.033	-0.033	-0.039	-0.040	-0.055	-0.037
pH				-0.382	0.205	-0.382	-0.033	-0.018	-0.327	-0.378	-0.350	-0.500	-0.421	-0.392
Cl ⁻					-0.566	0.984	-0.259	-0.666	0.966	0.998	0.990	0.799	0.977	0.918
HCO ₃ ⁻						-0.519	0.371	0.578	-0.503	-0.558	-0.554	-0.427	-0.542	-0.452
SO ₄ ²⁻							-0.164	-0.615	0.974	0.983	0.984	0.785	0.953	0.946
NO ₃ ⁻								0.478	-0.226	-0.260	-0.275	-0.017	-0.199	-0.229
SiO ₂									-0.585	-0.666	-0.662	-0.488	-0.657	-0.570
B										0.974	0.987	0.656	0.896	0.924
Na ⁺											0.995	0.774	0.968	0.921
K ⁺												0.723	0.942	0.924
Ca ²⁺													0.894	0.754
Mg ²⁺														0.884

and 13 come from wells situated over metapelitic deposits, where there is little influence of marine intrusion; on the other hand, samples 2, 3, 5 and 8 (and less obviously sample 4) come from the western sector

of the detrital aquifer and close to the coast. Analysis of these samples gave higher values of SO₄²⁻/Cl⁻ and Sr²⁺ and lower values of the Mg²⁺/Ca²⁺ ratio, which indicates a longer residence time of the groundwater.

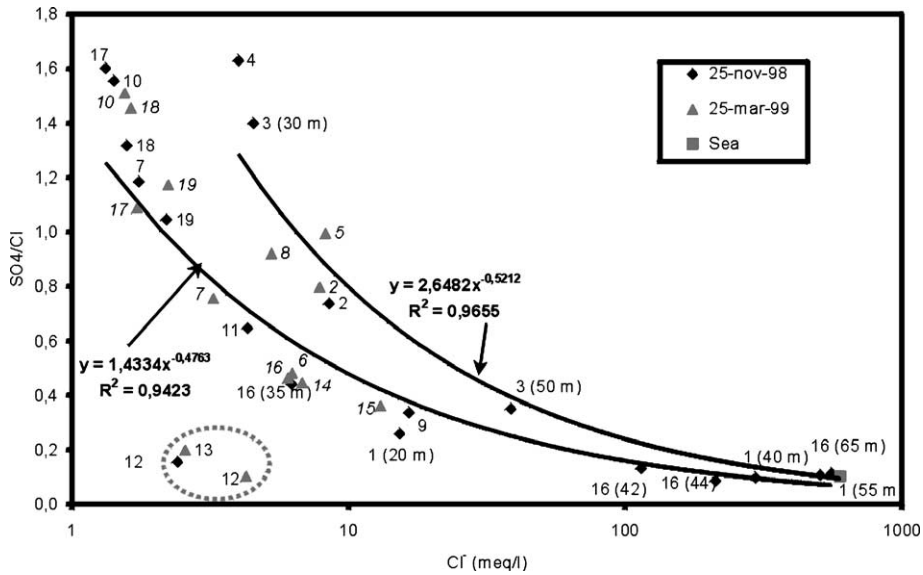


Fig. 4. $\text{SO}_4^{2-}/\text{Cl}^-$ (in meq/l) as a function of the Cl^- content (meq/l) in the different samples.
 Fig. 4. Rapport $\text{SO}_4^{2-}/\text{Cl}^-$ en fonction de la teneur en Cl^- (meq/l) des différents points d'eau.

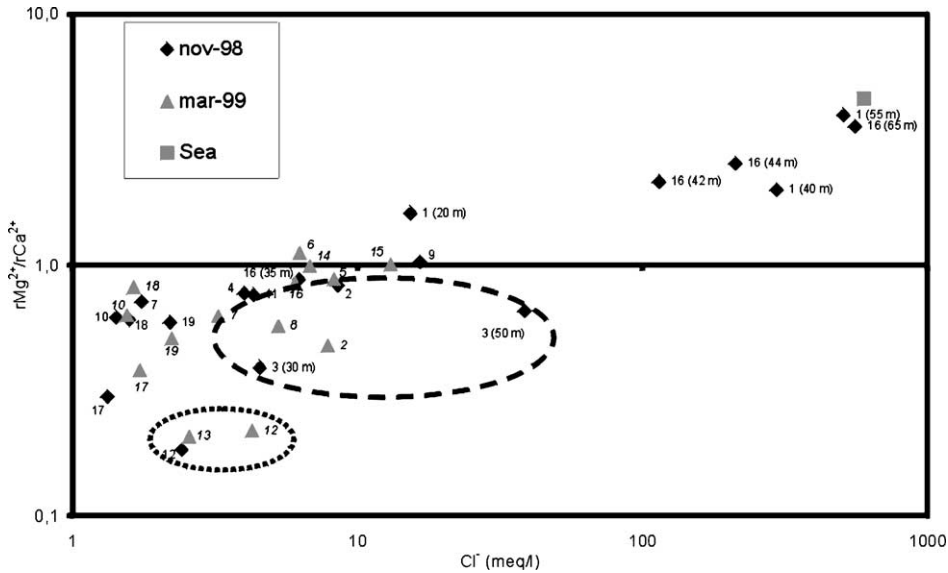


Fig. 5. $\text{Mg}^{2+}/\text{Ca}^{2+}$ ratio as a function of the Cl^- content (meq/l) in the different samples.
 Fig. 5. Rapport $\text{Mg}^{2+}/\text{Ca}^{2+}$ en fonction de la teneur en Cl^- (meq/l) des différents points d'eau.

This extended contact leads to a greater dissolution of the gypsum present in the metapelitic as well as of the carbonate cement present in the detritic layers of the aquifer, so providing an additional input of Sr^{2+} . The longer residence time also favours cation exchange

between Ca and Na, so that the concentration of dissolved Ca is lower.

This longer residence time deduced in these samples is explained by the existence of two zones of differing transmissivity in the coastal section of the

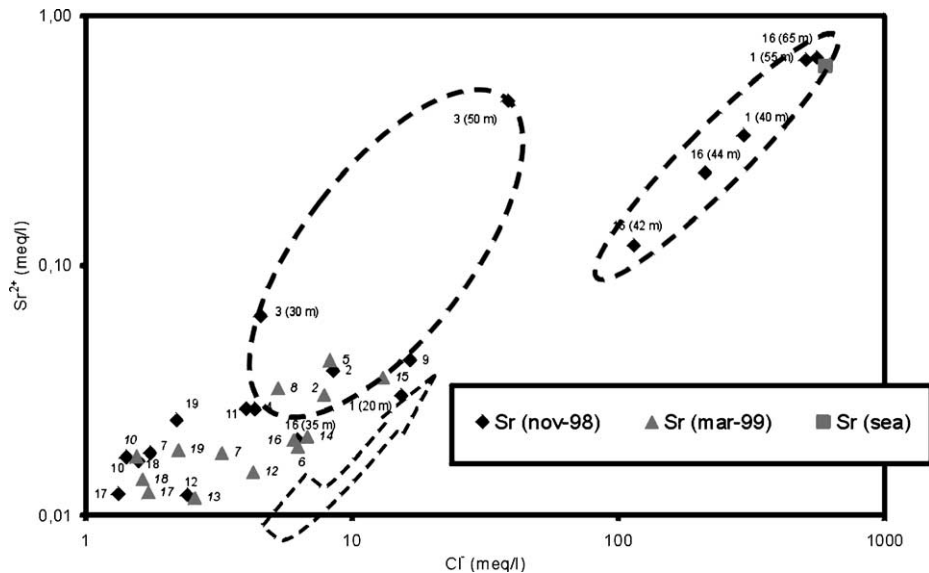


Fig. 6. Dissolved Sr^{2+} (meq/l) as a function of the Cl^- content (meq/l) in the different samples.

Fig. 6. Sr^{2+} dissous (meq/l) en fonction de la teneur en Cl^- (meq/l) des différents points d'eau.

aquifer, which also shows different patterns of groundwater circulation. There is a preferential flowpath along which water flows in either direction due to the elevated transmissivity of the material (karstified massif of Castell de Ferro). In addition, there is a secondary flowpath (Fig. 7) along which flow is slower and less abundant as a result of its lower transmissivity and longer extent (western detrital sector) [6]. Marine intrusion could take place along either sector but is more significant along the preferential flowpath. Flow in the opposite direction, i.e., aquifer flushing, will also occur through both sectors, although the western detrital sector is always more contaminated than the preferential path. As a result, both sectors will exhibit fresh water-seawater mixing, but the different residence times will impart distinct hydrogeochemical characteristics on each sector, as highlighted by the results of this study.

5. Conclusions

Consideration of the $\text{SO}_4^{2-}/\text{Cl}^-$ and $\text{Mg}^{2+}/\text{Ca}^{2+}$ ratios and Sr^{2+} content has allowed the differentiation of three groups of water in the Castell de Ferro aquifer. The smallest group of samples has very low $\text{SO}_4^{2-}/\text{Cl}^-$ and $\text{Mg}^{2+}/\text{Ca}^{2+}$ ratios and Sr^{2+} content.

These samples do not show any evidence of a marine origin. The other two groups indicate differing residence times. The smaller of these two groups shows high $\text{SO}_4^{2-}/\text{Cl}^-$ and Sr^{2+} , indicating a longer contact time between the water and rock which enables the dissolution of small gypsiferous fractions that are dispersed throughout the aquifer. The low $\text{Mg}^{2+}/\text{Ca}^{2+}$ ratio is interpreted as being due to the existence of inverse cation exchange, which withdraws Ca^{2+} and gives Na^+ to the solution. The prolonged contact time with the rock is due to the lower transmissivity of the part of the aquifer where these wells and boreholes are found. In this way, the principal flow in the aquifer occurs through the strata that are more transmissive than those occurring along the coastal fringe. However, to the west of the massif is a zone comprising detrital sediments that are beyond this preferential flowpath; here the groundwater flowing in from the sea or from the land remains in contact with the aquifer matrix for a longer time than in the remainder of the aquifer. A third group indicates ionic ratios and Sr^{2+} content that are considered normal for the process of mixing between salt- and fresh water. Though the existence of a preferential flowpath through the carbonate block has been previously highlighted using hydrodynamic criteria [7], the results obtained in this hydrogeochem-

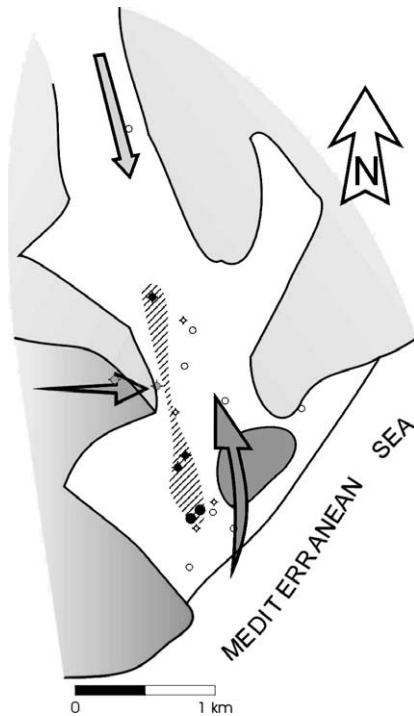


Fig. 7. Scheme of the behaviour of the Castell de Ferro aquifer. The arrows indicate the direction of flow of waters with a greater or lesser salt content according to the intensity of colour given. The hatched area represents the area of lower transmissivity, detected from the water chemistry. The wells represented by a shaded symbol are those that enabled this area to be detected, whilst the remainder are shown unshaded.

Fig. 7. Schéma du fonctionnement de l'aquifère de Castell de Ferro. Les flèches indiquent les sens de flux des eaux à teneur saline plus ou moins élevée, selon l'intensité de la couleur de l'intérieur. La zone rayée représente le secteur de moins grande transmissivité, détecté à partir de la chimie de l'eau. Les puits remplis sont ceux qui ont permis de détecter cette zone, tandis que ceux qui sont vides représentent les autres puits.

ical study serve to confirm the theory from a different viewpoint.

Acknowledgements

This investigation was partially financed by the CICYT Projects AMB 095-0495 and HID99-0597-CO2-02. We are grateful for the help of Maïthé Leboeuf during the second sampling survey. We also are grateful to the reviewers for their interesting

comments, which enabled us to make improvements to the original manuscript.

References

- [1] F. Aldaya, Mapa geológico y memoria explicativa de la hoja 1056 (Albuñol) del Mapa Geológico de España a escala 1:50 000, IGME, Madrid, 1981.
- [2] C.A.J. Appelo, D. Postma, *Geochemistry, Groundwater and Pollution*, Balkema, Rotterdam, 1993.
- [3] J. Benavente, *Las aguas subterráneas de la Costa del Sol de Granada*, Univ. Granada-Dip. Prov. Granada, 1985.
- [4] J. Benavente, Consecuencias de la sobreexplotación en el acuífero costero de la rambla de Gualchos (Granada), *Hidrogeol. y Rec. Hidrául.* XI (1987) 685–697.
- [5] M.L. Calvache, *Simulación matemática del contacto agua dulce-agua salada en algunos acuíferos de la Costa del Sol*, PhD Thesis Univ. Granada, 1991.
- [6] M.L. Calvache, A. Pulido-Bosch, Modeling the effects of salt-water intrusion dynamics for a coastal karstified block connected to a detrital aquifer, *Ground Water* 32 (5) (1994) 767–777.
- [7] M.L. Calvache, A. Pulido-Bosch, Processus d'extrusion-intrusion marine dans des aquifères côtiers du Sud de l'Espagne, *C. R. Acad. Sci. Paris, Sér. Ila* 323 (1996) 673–679.
- [8] M.L. Calvache, A. Pulido-Bosch, Effects of geology and human activity on the dynamics of salt-water intrusion in three coastal aquifers in southern Spain, *Environ. Geol.* 30 (3/4) (1997) 215–223.
- [9] B.F. Jones, A. Vengosh, E. Rosenthal, Y. Yechieli, Chapter 3: *Geochemical Investigations*, in: J. Bear, A.H.D. Cheng, S. Sorek, D. Ouazar, I. Herrera (Eds.), *Seawater Intrusion in Coastal Aquifers – Concepts, Methods and Practices*, Kluwer Academic Publishers, Dordrecht, The Netherlands, 1999, pp. 51–72.
- [10] A. Pulido-Bosch, I. Morell, J.M. Andreu, Modifications hydrogéochimiques provoquées par la surexploitation d'un aquifère karstique, *C. R. Acad. Sci. Paris, Sér. Ila* 323 (1996) 313–318.
- [11] P. Pulido-Leboeuf, *Contribución al conocimiento de acuíferos costeros complejos. Caso de Castell de Ferro*, Tesis Licenciatura Univ. Granada, 2000.
- [12] J.H. Tellam, J.W. Lloyd, Problems in the recognition of seawater intrusion by chemical means: an example of apparent equivalence, *Q. J. Eng. Geol.* 19 (1986) 389–398.
- [13] L. Tulipano, M.D. Fidelibus, Geochemical characteristics of Apulian coastal springs water (Southern Italy) related to mixing processes of groundwaters with sea water having different residence time into the aquifer, in: *Proc. 5th Int. Conf. Water Resources Planning and Management*, Athens, 1984, pp. 2.55–2.67.
- [14] A. Vengosh, E. Rosenthal, Saline groundwater in Israel: its bearing on the water crisis in the country, *J. Hydrol.* 156 (1994) 389–430.